JOURNAL OF AIRCRAFT
Vol. 41, No. 6, November–December 2004

Engineering Notes

ENGINEERING NOTES are short manuscripts describing new developments or important results of a preliminary nature. These Notes cannot exceed 6 manuscript pages and 3 figures; a page of text may be substituted for a figure and vice versa. After informal review by the editors, they may be published within a few months of the date of receipt. Style requirements are the same as for regular contributions (see inside back cover).

Effects of Wing and Canard Sweep on Lift Enhancement of Canard Configurations

Bao-Feng Ma,* Pei-Qing Liu,† and Yuan Wei‡
Beijing University of Aeronautics and Astronautics, 100083 Beijing, People's Republic of China

Nomenclature

Re	=	Reynolds number based on wing root chord
α	=	angle of attack, deg
ΔC_L	=	lift coefficient difference between the canard configuration and delta wing (baseline configuration)
Λ_C	=	canard sweep angle, deg
Λ_W	=	wing sweep angle, deg

Introduction

BEHRBOHM[1] first found in 1965 that a close-coupled canard configuration has substantial advantages: Adding a canard to the wing increases the maximum lift coefficient and delays the stall angle of attack. This advantage mainly results from favorable interference between the canard and wing. From then on, many experimental studies have been conducted on a close-coupled canard configuration. These studies are roughly divided into two categories by research objective: one is parametric studies based on force measurement to find practical configurations,[2–9] and the other is flow mechanism studies of lift enhancement based on pressure measurement, flow visualization, etc.[10–21]

Whichever category the study belongs to, the wing and canard sweep angle is usually an important parameter worthy of study. Of modern high-maneuverability aircraft, the wing and canard usually adopts delta wings. Previous work indicated that the sweep angle of the delta wing was very important parameter that seriously affects the delta-wing lift characteristics and flow patterns. Thus, with regard to the delta-wing/canard configuration, it was learned that the wing and canard sweep angle would affect lift-enhancement characteristics and wing/canard vortex interference modes. However, the studies did little to teach researcher how to affect these characteristics. The previous studies mainly focused on the canard sweep effect, whereas the wing sweep was basically fixed.[3,7,12,13,18] No study was carried out covering the effect on lift enhancement when both delta-wing and canard varied from low to high sweep angles.

Received 2 March 2004; revision received 30 March 2004; accepted for publication 30 March 2004.

*Ph.D. Candidate, Institute of Fluid Mechanics; BaofengMa@hotmail.com.
†Professor, Institute of Fluid Mechanics; bhlpq@263.net.
‡Graduate Student, Institute of Fluid Mechanics.

Thus, in the present Note, a detailed study will be made on the effect of the wing's and canard's sweep angles on lift enhancement of a delta-wing/canard configuration at low to high incidence by force measurement. The wing sweep varies from 40 to 75 deg and the canard sweep varies from 40 to 80 deg.

Experimental Setup

The experiment was conducted in the D1 wind tunnel of Beijing University of Aeronautics and Astronautics, which had a 1.02×0.76 m ellipse-shaped test section with 2-m length. The freestream turbulence intensity was less than 0.3%.

There were 72 delta-wing/canard configurations made of nine canards and eight wings used in the present experiment. The canard area is 12.25% of that of the wing. All canards have an identical area and so do all wings. The canard sweep angles are 40–75 deg at 5-deg intervals and the wing sweep angles are 40–80 deg at 5-deg intervals. The wing and canard are coplanar, and the longitudinal distance between them is zero. They are made of organic glass with 3-mm thickness and a leeward-beveled 45-deg angle. One of the canard-configuration models is shown in Fig. 1.

A six-component balance was used to measure lift force from -1.6 to 48.4 deg angle of attack. The experimental maximum-blockage-degree is less than 0.9%. The incoming velocity is 20 m/s, and the corresponding Reynolds numbers based on the delta-wings' root-chord length are 2.0×10^5–4.0×10^5.

The mean-square-root errors of seven repeated experiments with a canard configuration of 40-deg sweep wing and 40-deg sweep canard is 0.0088 for lift coefficient. The model angle of attack can be set to within 0.05 deg.

Results and Discussion

The lift-coefficient calculation of the delta wing (baseline configuration) adopts the wing area as a reference area, but the reference area of the canard configurations is the sum of the wing area and the canard area. Thus, the effect of adding the canard area can be eliminated, and the lift enhancement will have more practical meaning. The final results are given by the lift-coefficient difference between the canard configuration and the corresponding baseline configuration.

At the low-to-moderate angles of attack, the canard configurations have no lift enhancement, regardless of how great the wings' and ca-

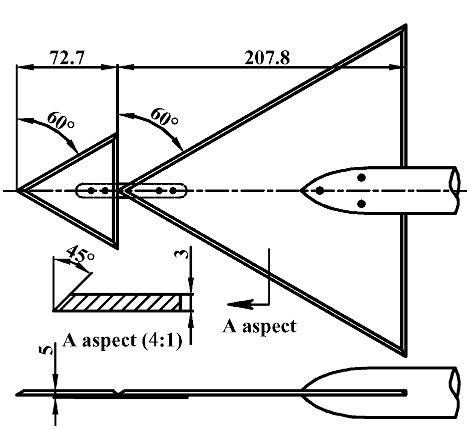

Fig. 1 Canard-configuration model.

nards' sweep angles are. Figures 2a and 2b respectively, presents the lift-coefficient increment (LCI) of the canard configurations at 8.4 and 18.4-deg angles of attack (AOA). From Fig. 2a, it can be seen that the LCI of all canard configurations is less than zero, which implies that no lift enhancement occurs. Figure 2b shows that only the canard configurations of 40-deg sweep wing have minor lift enhancement when the canard sweep is from 50 to 65 deg. Of the canard configuration of 45-deg sweep wing and 50-deg sweep canard, the LCI is also more than zero. However, the increments are very small and can even be neglected if the experimental error is considered.

Figure 2c presents the LCI at 23.4-deg AOA. Note that both LCI curves of 40- and 45-deg sweep wing have lift enhancement in the whole range of canard sweep, and they both reach the maximum increment value at 80-deg canard sweep angle. The LCI curve of 50-deg sweep wing begins to rise across the zero-increment line ($\Delta C_L = 0$) and already almost lies over it. Nevertheless, the LCI curves of sweep wings greater than 50-deg are still located under the zero-increment line.

Figure 2d shows LCI at 28.4-deg AOA. The LCI curves over the zero-increment line have become three pieces. The variation of the three curves with canard sweep angle is very similar, and they all reach the maximum value at 75-deg canard sweep angle. The canard configurations of 40-deg sweep wing have the best results from lift enhancement. The canard configurations of 45-deg sweep wing are the second. Those of 50-deg sweep wing are the third. The LCI curve of 55-deg sweep wing has gone partly across the zero-increment line, and the LCI curves of more than 55-deg sweep wing are still located under the zero-increment line.

For a 30.4-deg AOA, the LCI is presented in Fig. 2e. Figure 2e is characterized by four pieces of curve located over the zero-increment line. Note that the canard configurations with 40-deg sweep wings end up with the best lift-enhancement effect, which is different from the preceding result. The canard configurations of 40–55 deg sweep wings have a better lift-enhancement effect at the canard sweep angles of 55–75 deg than at the other canard sweep angles. The canard configurations of 60–75 deg sweep wing have no lift enhancement at this AOA.

Figure 2f shows the LCI at 38.4-deg AOA. Note that the LCI curves over the zero-increment line have increased to five pieces, and only the LCI curves of 65-, 70-, and 75-deg sweep wings lie under the zero-increment line. The LCI curves of 40-, 45-, 50-, and 55-deg sweep wings reach the maximum value at 65-deg canard

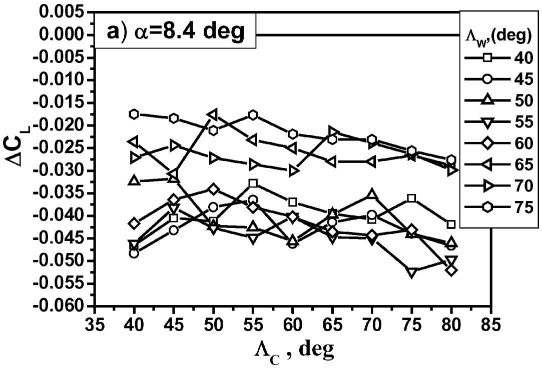

Fig. 2a ΔC_L **vs** Λ_C **for canard configurations of different sweep wings.**

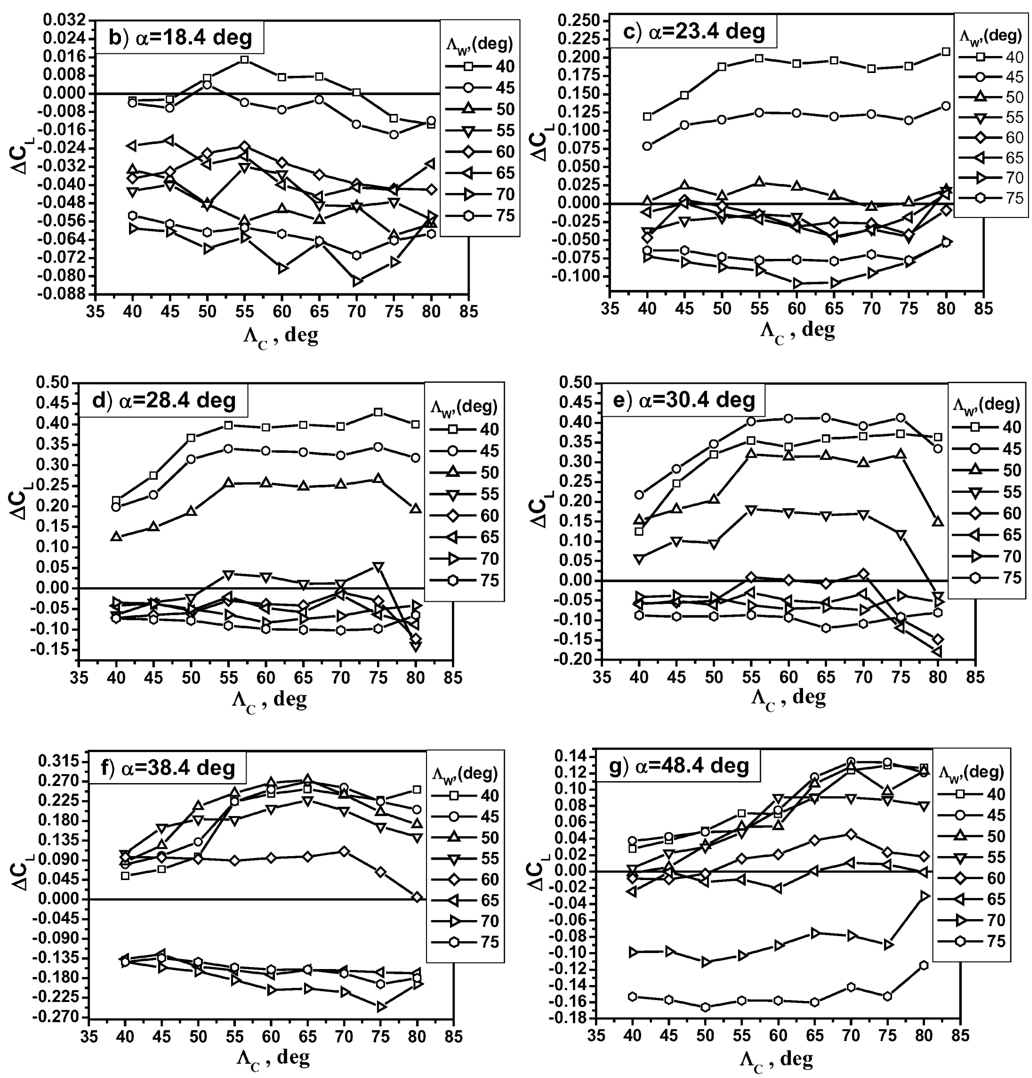

Figs. 2b–2g ΔC_L **vs** Λ_C **for canard configurations of different sweep wings.**

sweep angle. As to the LCI curve of the 60-deg sweep wing, the LCI basically remains constant when the canard sweep angles are between 40 and 70 deg.

Figure 2g shows the LCI at 48.4-deg AOA. Note that the LCI curve of the 65-deg sweep wing has approached the zero-increment line and lies partly over it. The LCI curves of the 40–55 deg sweep wing approximately increase with canard sweep angles when the canard sweep is less than 70 deg and arrive at a maximum value at a 70-deg canard sweep angle. The LCI curve of the 60-deg sweep wing arrives at a maximum value at a 70-deg canard sweep angle. In addition, when the canard sweep is 40 or 45 deg, the LCI of the 60- and 65-deg sweep wings become lower than zero. The canard configurations of 70- and 75-deg sweep wings have no lift enhancement at this AOA.

Conclusions

Under the conditions of the present experiment, the lift enhancement of canard configurations is substantially affected by the wing sweep and AOA. When AOA is less than a certain critical value, no lift enhancement occurs on any canard configurations. When AOA is more than the critical value, the canard configurations of the 40-deg sweep wing are the first to have a lift-enhancement effect. As the wing sweep of canard configurations becomes larger, the AOA at which lift-enhancement occurs becomes larger. At certain AOA, generally speaking, the canard configurations of the lower sweep wings have a greater benefit from the effect of lift enhancement. With regard to the canard configurations of certain sweep wings having lift enhancement effect, the effect of the canard sweep on the lift enhancement varies with AOA, but at each AOA, an optimum canard sweep for lift enhancement exists.

References

[1]Behrbohm, H., "Basic Low Speed Aerodynamic of Short-Coupled Canard Configuration of Small Aspect Ratio," SAAB TN-60, Linkoping, Sweden, July 1965.

[2]Gloss, B. B., "Effect Of Canard Location and Size on Canard–Wing Interference and Aerodynamic Center Shift Related to Maneuvering Aircraft at Transonic Speeds," NASA TN-D-7505, June 1974.

[3]Gloss, B. B., "The Effect of Canard Leading-Edge Sweep and Dihedral Angle on the Longitudinal and Lateral Aerodynamic Characteristics of a Close-Coupled Canard–Wing Configuration," NASA TN-D-7814, Dec. 1974.

[4]Gloss, B. B., "Effect of Wing Planform and Canard Location and Geometry on the Longitudinal Aerodynamic Characteristics of a Close-Coupled Canard–Wing Model at Subsonic Speeds," NASA TN-D-7910, June 1975.

[5]Re, R. J., and Capone, F. J., "Longitudinal Aerodynamic Characteristics of a Fighter Model With a Close-Coupled Canard at Mach Numbers from 0.40 to 1.20," NASA TP-1206, July 1978.

[6]Lacey, D. W., and Chorney, S. J., "Subsonic Aerodynamic Characteristics of Closed-Coupled Canards with Varying Area and Position Relative to a 50° Swept Wing," U.S. Naval Ship Research and Development Center, TN AL-199, West Bethesda, MD, March 1971.

[7]Lacey, D. W., "Aerodynamic Characteristics of the Closed-Coupled Canard as Applied to Low-to-Moderate Swept Wing," U.S. Naval Ship Research and Development Center, Aeronautical Rept. 1256, West Bethesda, MD, Jan. 1979.

[8]Krouse, J. R., "Effects of Canard Planform on the Subsonic Aerodynamic Characteristics of a 25° and a 50° Swept Wing," U.S. Naval Ship Research and Development Center, Evaluation Rept. AL 91, West Bethesda, MD, May 1972.

[9]Ottensosor, J., "Wind-Tunnel Data on the Transonic Aerodynamic Characteristics of Closed-Coupled Canards with Varying Planform, Position and Deflection Relative to 50° Swept Wing," U.S. Naval Ship Research and Development Center, Test Rept. AL 88, West Bethesda, MD, May 1972.

[10]Gloss, B. B., and Washburn, K. E., "Load Distribution on a Close-Coupled Wing Canard at Transonic Speeds," *Journal of Aircraft*, Vol. 15, No. 4, 1978, pp. 234–239.

[11]Stoll, F., and Koenig, D. G., "Large-Scale Wind-Tunnel Investigation of a Close-Coupled Canard-Delta-Wing Fighter Model Through High Angles of Attack," AIAA Paper 83-2554, Oct. 1983.

[12]Er-El, J., and Seginer, A., "Vortex Trajectories and Break Down on Wing–Canard Configurations," *Journal of Aircraft*, Vol. 22, No. 8, 1985, pp. 641–648.

[13]Er-El, J., "Effect of Wing/Canard Interference on the Loading of a Delta Wing," *Journal of Aircraft*, Vol. 25, No. 1, 1988, pp. 18–24.

[14]Oelker, H. C., and Hummel, D., "Investigation on the Vorticity Sheets of a Close-Coupled Delta–Canard Configuration," *Journal of Aircraft*, Vol. 26, No. 7, 1989, pp. 657–666.

[15]Hummel, D., and Oelker, H. C., "Low-Speed Characteristics for the Wing–Canard Configuration of the International Vertex Flow Experiment," *Journal of Aircraft*, Vol. 31, No. 4, 1994, pp. 868–878.

[16]Erickson, G. E., Schreiner, J. A., and Rogers, L. W., "Canard–Wing Vortex Interaction at Subsonic Through Supersonic Speeds," AIAA Paper 90-2814, Aug. 1990.

[17]Thompson, D. H., "Visualization in Water of Vortex Flow Over Sharp-Edged Canard Configurations," Aeronautical Research Lab., ARL-FLIGHT-MECH-R-189, Victoria, Australia, April 1992.

[18]Ponton, A. J., Lowson, M. V., and Barrett, R. V., "The Evaluation of Canard Couplings at High Angles of Attack," AIAA Paper 92-0281, Jan. 1992.

[19]Howard, R. M., and Kersh, J. M., "Effect of Canard Deflection on Enhanced Lift for a Close-Coupled-Canard Configuration," AIAA Paper 91-3222, Sept. 1991.

[20]Howard, R. M., and O'Leary, J. F., "Flowfield Study of a Closed-Coupled Canard Configuration," *Journal of Aircraft*, Vol. 31, No. 4, 1994, pp. 908–914.

[21]Bergmann, A., and Hummel, D., "Aerodynamic Effect of Canard Position on a Wing Body Configuration in Symmetrical Flow," AIAA Paper 01-0116, Jan. 2001.